

2021

Effect of surface profile on axial load transfer mechanism of tendons

Ashkan Rastegarmanesh
University of Southern Queensland

Joel Misa
Noma Consulting

Ali Mirzaghobanali
University of Southern Queensland

Naj Aziz
University of Wollongong

Kevin McDougall
University of Southern Queensland

Follow this and additional works at: <https://ro.uow.edu.au/coal>

Recommended Citation

Ashkan Rastegarmanesh, Joel Misa, Ali Mirzaghobanali, Naj Aziz, and Kevin McDougall, Effect of surface profile on axial load transfer mechanism of tendons, in Naj Aziz and Bob Kininmonth (eds.), Proceedings of the 2021 Resource Operators Conference, Mining Engineering, University of Wollongong, 18-20 February 2019
<https://ro.uow.edu.au/coal/827>

EFFECT OF SURFACE PROFILE ON AXIAL LOAD TRANSFER MECHANISM OF TENDONS

Ashkan Rastegarmanesh^{1*}, Joel Misa², Ali Mirzaghobanali³, Naj Aziz⁴ and Kevin McDougall³

ABSTRACT: Cable bolts as one of the most common means of ground support in surface and underground projects are attracting more attention due to their advantages over more expensive and cumbersome support elements. Thus, newer cables with new configurations and surface properties are emerging on a regular basis. Conventionally, the performance of cable bolts is studied in two main categories of axial and shear load transfer mechanisms. This paper focuses on the former by developing and proposing an experimental plan to cast light on the effect of surface profile on axial performance of cable bolts. Consequently, 15 representative surface profiles were designed and machined on metal base plates using a CNC machine. Later, these plates were used as moulds for casting cylindrical samples of Stratabinder cementitious grout. Three curing times of one day, 7 days, and 28 days were studied under static compression loading. It was observed that the surface roughness of the samples plays a major role in failure as it inhibits free movement of grout metal interface and inflicts end effect as well as introducing stress concentration point. These two drastically reduce the performance of grout and cause tensile crack growth.

INTRODUCTION

Tendons are extensively used in civil and mining projects across Australia to support underground structures (Bajwa et al., 2017). In highly stressed ground conditions, tendons become the dominant form of ground support. Tendons are a type of rock reinforcement used to stabilise the rock mass during tunnel excavations (Figure). Tendons transfer the load of the unstable rock mass to the much stronger interior rock mass through the grout. This transfer occurs as a direct result of cohesion and friction between the bolts and the grout. The grout then transferred the loads to the surrounding rocks (Hutchinson et al., 1996).

Grouts are blended cementitious powder when mix with water would act as a high strength bonding agent. It is easily pumpable on the hole. The tendons are normally installed in a patterned spaced borehole to provide reinforcement and support for the wall and roof of an underground excavation floor (Figure 2).

The tendon-grout interface's normal load behaviour and failure mechanism are of great significance for load transfer capacity and design of the rock bolting and cable bolting system (Zhang et al., 2020). Improvement of the tendons' surface geometry significantly improves the tendons' load transfer efficiency and anchorage capacity. This research is intended to investigate the effects of the tendon surface profile and curing time of grout on normal load transfer mechanisms of rock reinforcing elements.

The experiment will replicate the normal load transfer between the rock formation and tendon/grout. A circular metal mould with different surface asperity will be cast with grout. After curing time, the specimen will be subjected to a continuous load until its structural integrity is compromised.

LITERATURE REVIEW

The underground primary support system aims to maintain the underground excavation open and safe for their required designed life span. It is achieved through the correct design and installation procedures of internal and external support and reinforcement system. The term tendons are used here in a generic sense and cover cable bolts and rock bolts as reinforcing elements. Tendons are either primarily frictional or fully coupled devices. Tendons prevent separation and slip along planes of

¹ Centre for Future Materials, University of Southern Queensland, QLD, Australia
Rastegarmanesh@gmail.com; Ashkan.Rastegarmanesh@usq.edu.au

² Head of Design Services, Noma Consulting, Australia

³ School of Civil Engineering and Surveying, University of Southern Queensland, QLD, Australia

⁴ School of Civil, Mining & Environmental Engineering, University of Wollongong, NSW, Australia

weakness in the rock mass. The design life of the tendons can range between 50 to 100 years. In Australia, the trend is to specify a 50 or 100 design life (Pells, et al., 1999).

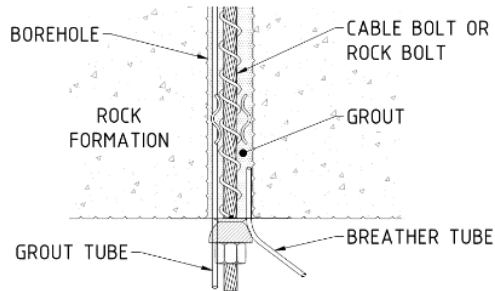


Figure 1: Typical Bolts Details

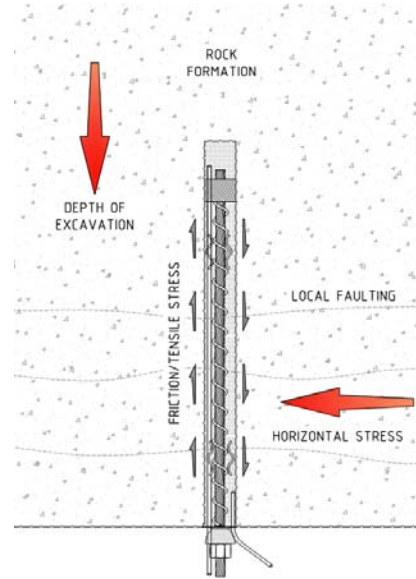


Figure 2: Typical Stress/Load Imposed on Tendon

Tendons can either be mechanically or manually installed in rock mass and tensioned to ensure all of the components are maintained in contact with and that a positive force is applied to the rock mass. Where the bolts are required to carry a significant load, it is generally recommended that a tension of approximately 70% of the capacity of the bolt be installed initially (Hoek, 2006). The load is transferred to or from the rock mass along their entire length unless debonded sections occur due to design or installation error. This transfer occurs as a direct result of friction between the tendons and the encapsulating grout. The load is then transferred to the surrounding rock mass (Hutchinson et al., 1996).

Hagan, et al., in 2014, released a paper on the load transfer mechanism of fully grouted cable bolts under laboratory tests. The author outlines the developments and evolution in understanding the load transfer mechanism of fully grouted cables under axial loadings. Three basic mechanisms provide the shear resistance; chemical adhesion, mechanical interlock, and friction. However, the influence of chemical bonding is only temporary. Hence in most cases, the mechanical interlock and friction dominate the effect of load transfer. The mechanical interlock is the relative movement between the cable bolt and cement grout, while friction occurs between the cable/grout interface preventing the cable from slipping. Modified cable bolt designs, such as the bulb on the strand, give a much higher load transfer capacity compared to conventional cables. Grout plays an integral part in keeping the tendons from failure due to corrosive environments. The grout must act as protection against corrosion. Longevity and sensitivity are an important consideration when cable bolts are exposed to corrosive environments, blasting, and changes in local stress and confinement (Hutchinson et al., 1996).

Also, grout serves to transfer load between the rock and the tendons. The essential properties of the grout to allow it to carry out its functions are strength and stiffness. These properties are functions of water to cement ratio (W/C), grout composition, and elapsed time since placement. For Portland cement grout Hyett, et al., (1992) found a decrease in both 28-day uniaxial compressive strength and deformation modulus with increasing water/cement ratio. Their results show that the properties of grouts with water/cement ratios of 0.35 to 0.4 are significantly better than those with ratios above 0.5. Majoor, et al., (2017) has studied the effect of the water-grout ratio. In their studies, the shear strength and UCS decrease as the water-grout ratio increases. The shear strength decreases by 27%, while the UCS decreases by 43%.

In 2016, Mirza, et al., conducted an extensive study the mechanical properties of two different grouts at various curing times using, the Jenmar Bottom-Up (BU100) and Orica Stratabinder HS. The experiment used a 50 mm cube mould with a mixing ratio of 5 and 7 litres/bag by weight of grout to water. All their samples failed in shear planes during compression tests. The named study was followed by Majoor, et al., in 2017 study of effect of the water to cement ratio on UCS and shear strength. They also performed triaxial testing to analyse the impact of confining pressures and obtain cohesion and internal friction angle values. The paper concluded that the water to grout ratio is a significant factor in both the uniaxial compressive strength and the shear strength of grout.

In 2018, Mirzaghobanali et al., conducted an extensive experiment on Orica Stratabinder HS using two different sample moulds, 70 mm cube mould, and 100 mm diameter x 200 mm high cylindrical mould. The samples were cured for 1, 7, 14, and 21 days and tested for UCS. The authors found out that the cube sample's UCS is higher than the cylindrical sample and the curing time has a significant effect on the samples' strength.

The bonding strength between the grout and rock and the grout and steel also plays a major role because they constitute the system's weakest points (Potvin et al., 1989). The surface profile of the tendons affects the stiffness of the bond strength between the tendon and grout. In Craig et al., (2012) study, the comparative laboratory testing determined that the nutcaged cables and indented wire cables provide stiffer and higher capacity bond strength than plain cable. The tendons' load transfer capacity is influenced by the shear strengths developed between the rock-grout and the grout-tendons interface interaction. In laboratory testing conducted by Aziz et al., (2006:2008), the grout-rock interface failure rarely occurs. The bonding strength between the grout-bolt interface dominates the effect of rock bolting.

Mechanical interlock is a critical component in load transfer capacity in rock bolting systems. The tendon profile configuration is the rib height, rib spacing, rib face angle, and rib cross-section shape. Cao et al., (2013) theorise that when an axial load is applied to cause the rock bolt's failure, the parallel shear failure, and dilational slip are the two major failure modes. Adding the Coulomb's shear failure criterion and the rock bolt's geometric profile to the equation, a universal upper limit of slipping angle can be calculated as the grout internal friction angle's complementary angle a more accurate result is achieved.

In 2006, Aziz, et al., experimented on the bolt surface configurations and load transfer mechanisms. Their experiment involves a laboratory test and numerical analysis. Using two types of bolts and two types of encapsulating steel sleeves for the laboratory pull and push test and ANSYS3D for the numerical simulation. They have concluded that the resin/bolt surface's load failure depends on the profile height and the spacing. The difference in grout material was studied by Pullan et al., (2018) and found both cement and resin grouts are both effective in load transfer. Their results indicated significant differences in the cable bolt's performance between being grouted in strong and weak material and little difference in the stiffness between all test scenarios.

In Zhang, et al., (2020) study result, there is a correlation between the bolt profile and grout mixture on the shear behaviour and failure mode under the constant normal load conditions. The results demonstrated the bolt-grout interface's shear behaviour is related to the profile, diameter, length of the rock bolts, and the grouting materials' mechanical properties and the boundary conditions. Failure in cable/grout interface was also observed by Bajwa et al. (2017), experiment whereby the plain strand cable profile offers a minimum amount of friction between the grout and cable compared to a modified cable bolt. This paper tries to replicate the axial load transfer mechanisms between the grout and tendons surface asperity under the tangential stress imposed on grout in situ.

METHODOLOGY

Specimen preparation

The two primary materials used in this experiment are aluminium mould and Minova Stratabinder HS grout. Minova Stratabinder HS is a high strength, anchoring grout. It is a blended cementitious grout. Supplied ready to use, and when mixed with water, it is free-flowing. Aluminium was chosen to be the metal/tendon material. Aluminium was chosen because it can easily be fabricated. Three-dimensional (3D) models of the sample moulds were produced using AutoCAD software. The specimen models are

then fabricated with a Computer Numerical Control (CNC) machine. There are a total of 15 tendon moulds with different asperities.

The tendon moulds have a base of 10 mm thick and a diameter of 63.5 mm (Figure 3). Figure 4 and Table 1 illustrate the mould's detail. It is worth mentioning that these patterns are not equivalent of the cables and bolts in the industry but rather were chosen as a representative of a smooth to an exaggerated rough surface condition. The other component of the specimen mould is a 65 mm diameter by 160 mm high PVC pipe. It forms the shape of the specimen. Figure 5 shows the set of PVC pipes used in the experiment. A heat gun shown in Figure 6 is used to widen the PVC pipe slightly so the tendon mould can be fitted inside the PVC pipe and form a tight fit to stop the seepage of the grout. The mixer shown in Figure 7 was to mix the grout mixture.



Figure 3: Tendon Mould

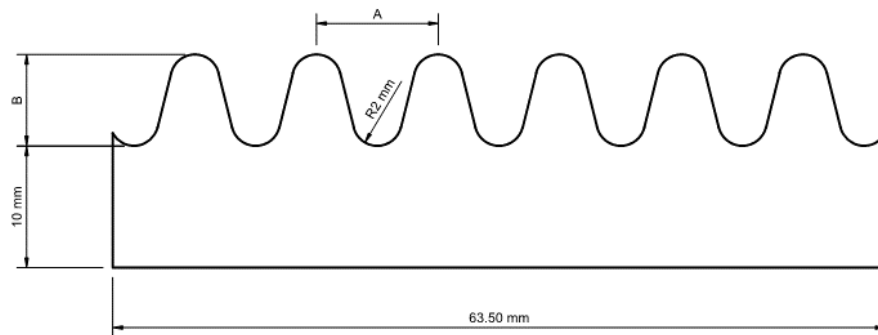


Figure 4: Tendon Mould Typical Cross Section



Figure 5: PVC Pipe



Figure 6: Heat Gun



Figure 7: Mixer

Table 1 illustrates the moulds' detail. It is worth mentioning that these patterns are not equivalent of the cables and bolts in the industry but rather were chosen as a representative of a smooth to an exaggerated rough surface condition.

Table 1: Surface Asperity

Mould name	A (width spacing mm)	B (height mm)
0 x 0	Flat surface	
6 x 2.5	6	2.5
6 x 5	6	5
6 x 7.5	6	7.5
10 x 2.5	10	2.5
10 x 5	10	5
10 x 7.5	10	7.5
10 x 10	10	10
15 x 2.5	15	2.5
15 x 5	15	5
15 x 7.5	15	7.5
15 x 10	15	10
20 x 2.5	20	2.5
20 x 5	20	5
20 x 7.5	20	7.5

Procedure in specimen preparation

1. The PVC pipe was cut to length, then heated using a heat gun to widen slightly, and then the tendon mould was inserted inside. The height to diameter ratio used is 2.5, according to ISRM recommendation.
2. A release agent (shuttering oil) was applied to the internal surface of the PVC pipe to facilitate the removal of the specimens; Making sure no oil is spilled on to the moulds. After applying oil on the pipe, the pipe is tip over, so the oil will not drip down the tendon mould as shown in Figure 8.
3. A grout mix is then prepared according to Minova's technical datasheet. Below is the calculation of the required grout mixture for the experiment

Table 2 Grout mix design (divided by three for easier mixing)

Water	Grout	Mixture
6 L	20 kg	12.5 L
1.22 L	4.05 kg	2.53 L

$$\begin{aligned} \text{Volume of grout mixture} &= 15 * \pi * \frac{63.5^2}{4} * 160 \\ &= 7.6 \times 10^6 \text{ mm}^3 \text{ or } 7.6 \text{ L} \end{aligned}$$

The breakdown of the 7.6 L grout mixture

$$\begin{aligned} \text{Grout weight} &= \frac{7.6 * 20}{12.5} \\ &= 12.16 \text{ kg of grout} \end{aligned}$$

$$\begin{aligned} \text{Litre of water} &= \frac{7.6 * 6}{12.5} \\ &= 3.65 \text{ L of water} \end{aligned}$$

For easy handling, the grout mixture was mixed in three batches (1.22L:4.05Kg)

1. The grout mixture was mixed, then poured into the specimen mould.
2. The grout mixture was tamped to make sure the grout mixture filled up the tendon mould's crevices. The PVC side was tapped slightly to release the entrapped air, then the top surface of the specimen mould was flattened to create an even surface. An even surface would distribute the load evenly to the specimen.
3. Once all 15 specimens have been cast, they were placed in the curing room for proper hydration and strength development. The specimens were cured at 1-day, 7-day, and 28-days strength.
4. A hack saw was used to remove the specimen from the PVC mould. This way, the integrity of the tendon-grout binding was preserved. The bond between the tendon and grout is sensitive due to the nature of the aluminium.
5. The specimens were marked using a marking pen, then the tested.
6. After testing, the tendon moulds were cleaned and prepared for the next curing time. The experiment was repeated three times for different curing periods.



Figure 8: specimen Mould Tip Over (marked)

Specimen testing

The specimens were tested using the SANS Universal Testing Machine (UTM) to determine the Uniaxial Compressive Strength (UCS) of the grout confined by the tendon mould at the bottom. The specimen was centrally mounted on the testing loading plate, and on top to remove the end friction effect. The load rate was maintained at at 1 m/min with the load being uniformly loaded until failure. Figure 9 and Figure 10 show the SANS UTM set up.



Figure 9: SANS machine



Figure 10: SANS data logger and control module

RESULT ANALYSIS

Experimental observations

The following notes were observed:

1. The specimen breaks before the grout reaches its peak UCS (Figure 11, Figure 12 and Figure 13).
2. The crack opening in the top part is wider. Figure 14, Figure 15 and Figure 16 are the 6x7.5 specimen at 1-day, 7-day & 28-day strength. As shown by the specimen, some icicle shape fragments are formed. The photos above imply that there is constrained from the bottom.
3. The line of failure is in a vertical direction or tensile mode. No shear mode failure was observed. Figure 17, Figure 18 and Figure 19 show the 10x2.5 specimen at 1-day, 7-day, and 28-day strength. As demonstrated by the specimen, all failures are tensile. Once the load is applied, the top portion of the specimen is free to move (expand), but mould constricts the specimen's bottom part creating this type of failure.
4. The initial cracks are parallel to the groove of the mould. Figure 20, Figure 21 and Figure 22 show the 10x7.5 specimen at 1-day, 7-day, and 28-day strength. As demonstrated by the specimen above, the cracks are parallel or align with the tendon mould's crevices or one can assume they initiate from the tip of the ridges due to stress concentration.



Figure 11: 6x5 specimen at 1-day strength



Figure 12: 6x5 specimen at 7-day strength



Figure: 13 6x5 specimen at 28-day strength

The UCS of the specimens were computed using SANS UTM's data output. The results are then tabulated and graphed. It was observed on the graph that the curved created was not a continuous curve path. There are intermittent drops in load applied as the specimen reaches its peak normal load or maximum UCS. Figure 23, Figure 24, Figure 25 and Figure 26 illustrate the results for 6 mm wide moulds in 1 day curing time period. The rest of the graphs all have the similar behaviour but with different failure load and displacement.

The peak normal load for specimen 10x2.5 in a 1-day strength test is 3.33 MPa, 8.95 MPa in a 7-day strength test, and 14.95 MPa in a 28-day strength test. The test result is below the strength in the technical data sheet of Minova Stratabinder HS of 50 MPa for 1-day, 78 MPa for 7-days, and 100 MPa for 28-days. The difference in results is attributed to, stress concentration and the end effect.

The poison effect of the normal stress on the top of the surface of the specimen causes the specimen to expand freely. Simultaneously, the mould restricted the same movement at the bottom part of the sample. The third factor was the stress concentration on the tip of the ridges on the aluminium moulds

which provided a place of onset of cracks. These three factors lend hand to create the failure pattern observed in these experiments (Figure 28).



Figure 14: 6x7.5 specimen at 1-day strength

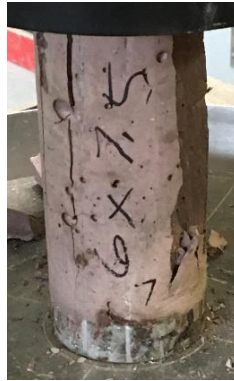


Figure 15: 6x7.5 specimen at 7-day strength



Figure 16: 6x7.5 specimen at 28-day strength



Figure 17: 10x2.5 specimen at 1-day strength



Figure 18: 10x2.5 specimen at 7-day strength



Figure 19: 10x2.5 specimen at 28-day strength

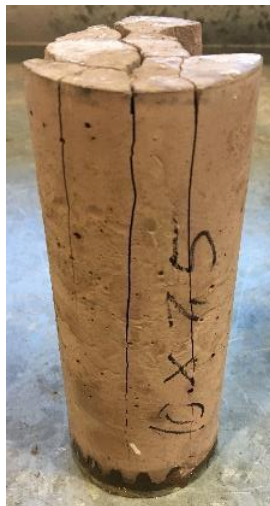


Figure 20: 10x7.5 specimen at 1-day strength



Figure 21: 10x7.5 specimen at 7-day strength



Figure 22: 10x7.5 specimen at 28-day strength

Figure 27 demonstrated the effect of the curing time on the specimen as the specimen is left to cure for a more extended period, the specimen peak normal load increases. The results indicated that the

height of asperity has a consistent effect on the specimen's strength compared to the asperity width. The higher the asperity, the higher the UCS of the specimen. The narrower the asperity width combined with lower asperity height, the lower specimen's UCS. As demonstrated in Figure 29, on a 1-day test and 28-day test, the specimen's UCS is higher when the height is 7.5mm. Reading the 7-day test result does not conform with earlier statements. To eliminate this phenomenon a more comprehensive experiment is required.

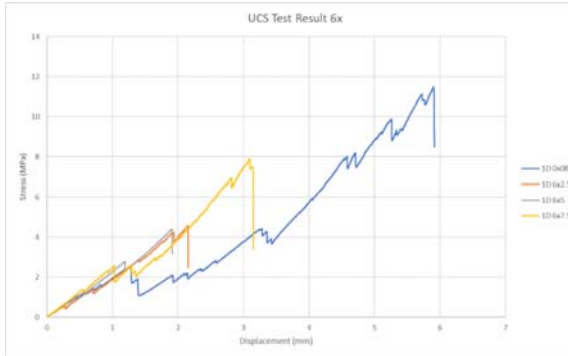


Figure 23: 6 mm wide 1 day results

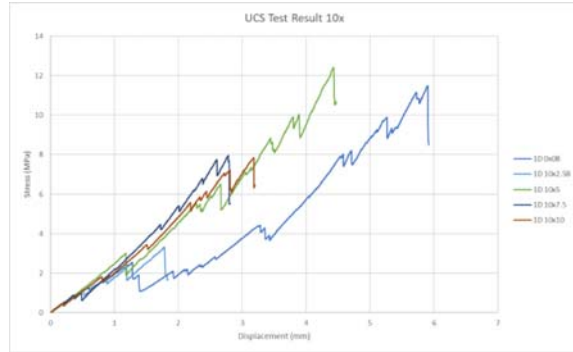


Figure 24: 10 mm wide 1 day results

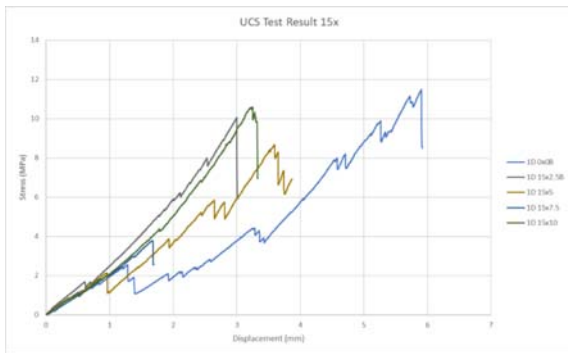


Figure 25: 15 mm wide 1 day results

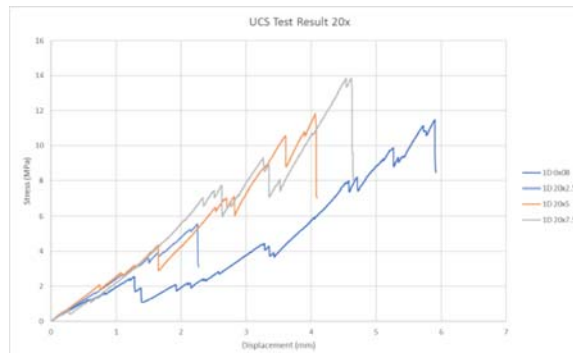


Figure 26: 20 mm wide 1 day results

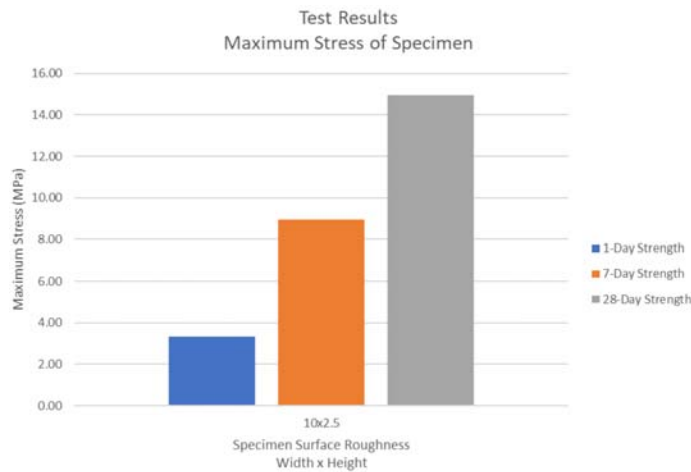


Figure 27: Test Results Maximum Stress of specimen

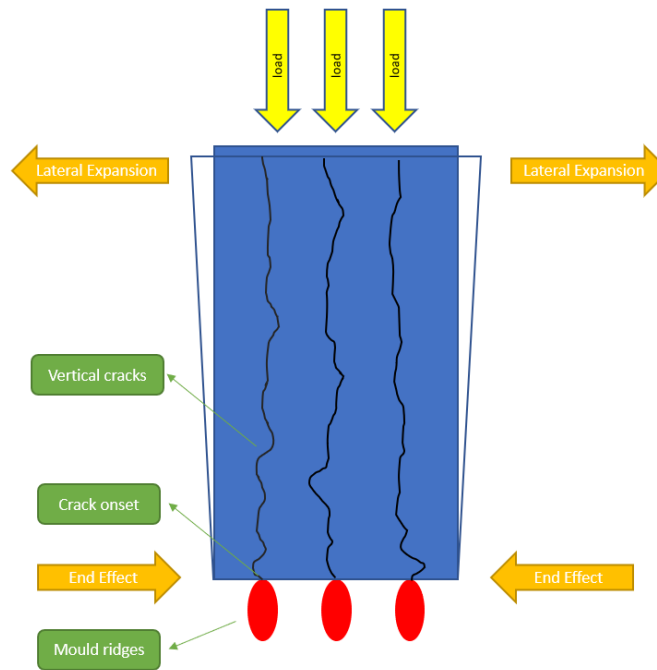


Figure 28: Failure theory



Figure 29: Test Results Maximum Stress specimen with 20mm Wide Asperity

In terms of the asperity's width, the results are inconclusive as there is no definite pattern that has emerged from the graphs. Although the narrow 6 mm wide asperity has the lowest UCS in the 1-day and 28-day test, it is not the case in the 7-day test. The 15x5 has the highest UCS in the 7-day and 28-day test (Figure 30). It is expected that the 20x5 specimen would have the highest UCS. It is recommended to conduct a more comprehensive experiment to determine the effect of the height.

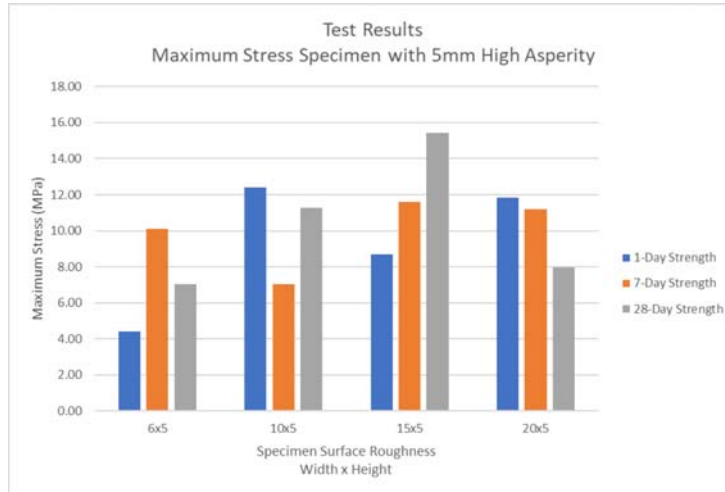


Figure 30: 5mm High Asperity Comparison

The secant modulus was computed using the first highest stress before the drop of stress and divide that by the strain. The results are tabulated and compared. In Figure 31, the effect of the curing time on the secant modulus is mixed. The experiment produced a contradictory result. Three of the specimens have conformed to the notion that the longer the curing time, the higher the secant modulus. The majority of the specimens have their highest secant modulus either in the 1-day test or 7-day test. The experiment result is inconclusive that the stiffness of the specimen increases as the curing time is longer.

The height and width of the surface asperity have an impact on the stiffness of the specimen. The calculated result produced is inconclusive. Figure 32 shows the comparison of the specimen with the same height of asperity with different width. The graph illustrated that on a 1-day test, the 15x2.5 specimen has the highest stiffness while on a 7-day test 6x2.5 specimen has the highest stiffness, but on a 28-day test, the 15x2.5 specimen has the highest stiffness. Further studies are recommended to determine the effect of the asperity on the stiffness of the tendon-grout specimen.

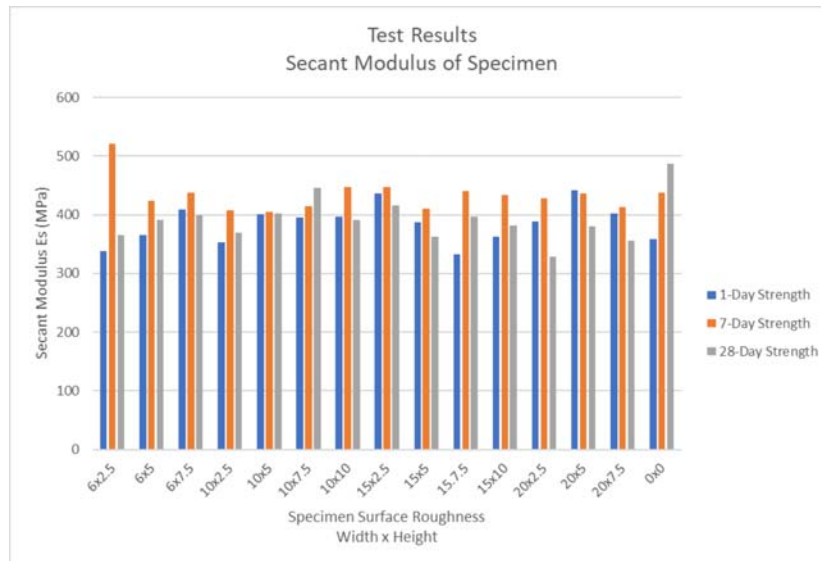


Figure 31: Test Results Secant Modulus

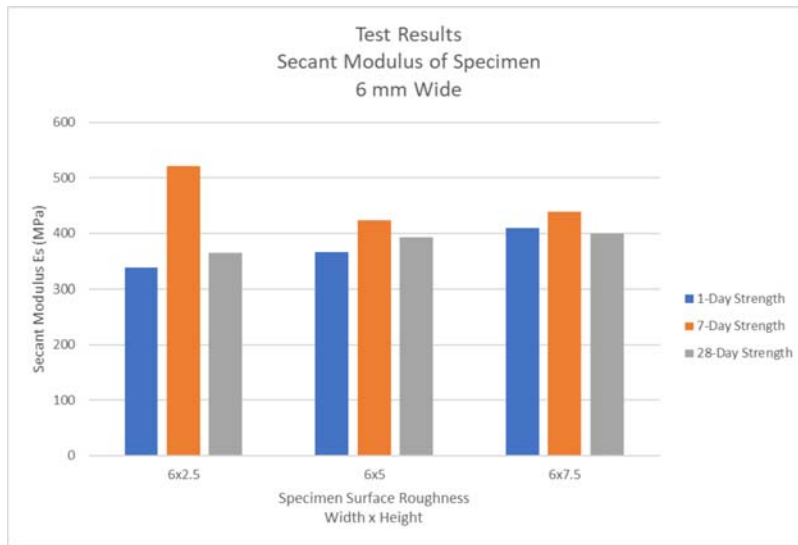


Figure 32: Wide specimen Comparison

Overall, the results produced conflicting results, especially with the 7-day test result producing some of the specimen's highest uniaxial compressive strength. Figure 33 summarises the test results across the three-day test. The 10x7.5 specimen in the 28-day test has the highest uniaxial compressive strength of 19.28 MPa, and the 6x2.5 specimen in the 28-day test has the lowest uniaxial compressive strength of 4.19 MPa. It was anticipated that the flat surface would have the highest uniaxial compressive strength, but the result did not reflect this.

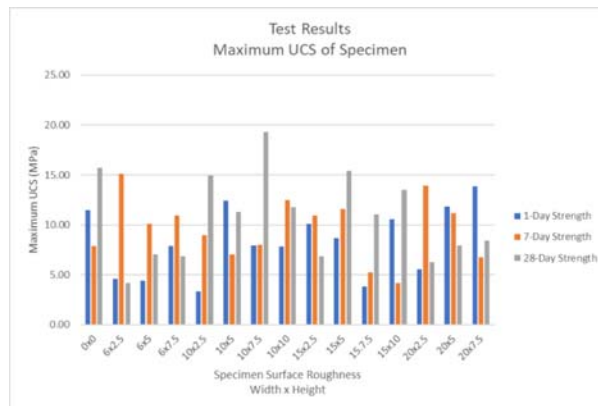


Figure 33: Test Results Maximum UCS of specimen

CONCLUSIONS

The following conclusions are inferred from the study

1. The tendon's normal load transfer mechanisms are influenced by the curing time and surface profile of the rock reinforcing elements. In general, the peak normal load increases with the increase in grout curing time. The uniaxial compressive strength of the specimen is higher at 28-day curing time. However, half of the results contradicted the expected outcome and suggested to carry out further studies.
2. The surface asperity also influences the stiffness and peak values of the normal load. In general, the peak normal load is lower as the height of asperity with the same width of asperity is lower. In the experiment, the 6x2.5 specimen has the lowest uniaxial compressive strength of 4.19 MPa, and the 10x7.5 specimen has the highest uniaxial compressive strength of 19.28 MPa. The study is inconclusive on the specific width and height of asperity. In theory, the

wider the asperity, the less restriction the grout to move, and the experiment did not prove this theory. In the comparison, the smaller the gap and lower the asperity's height, the lower the uniaxial compressive strength based on the 28-day curing time. Overall, the effect of the asperity on the grout's UCS is significant.

3. Comparing the results obtained to Mirzaghobanali's 2017 work on cube mould and cylindrical mould, the maximum UCS obtained is 442% below the cube mould UCS and 373% below the cylindrical mould. It is noted in the named study experiment is an unconfined test whereby both ends of the samples are free to move or expand. In contrast, this experiment has one end confined by the tendon's mould asperity. That restricts the bottom end from expanding or moving, also causing a tensile plane mode of failure.
4. The stiffness of the tendon-grout specimen is inconclusive in this experiment. The surface asperity has a definite impact on the stiffness of the specimen. Still, it is inconclusive to determine which portion of the asperity impacts whether the height or width has the most impact. The curing time also affects the stiffness, although the experiment did not produce the desired outcome. Some specimens demonstrated the desired effect of the curing time, such as 0x0, 10x5, 10x7.5. The longer the specimen is cured, the stiffer it gets.
5. Aluminium does not reflect the tendon's material. Furthermore, it proved to be more susceptible to losing its bond to the grout prior to the tests. Lastly, due to soft nature of aluminium, cleaning of the moulds is not easy. Yet, a CNC machine takes a considerably more time to machine a steel mould which may make the aluminium compromise worth it,
6. Lubricating the PVC pipes may cause the oil to be washed down by the grout to the metal mould in the bottom. This will cause a thin layer of oil to be form between the contact of mould and grout which will weaken the bond. Once the oil is applied in the inside face of the PVC pipe, it is highly recommended to tip over the specimen's mould. Also, the amount of the oil should be extremely limited or perhaps completely removed from the experiment.
7. Due to the small size of the samples the usual grout mixing precautions should be applied. For instance, the samples are significantly sensitive to the condition of the grout (fresh bags or badly sealed bags), water content in the mix, proper even mixing, tapping and disturbing the sample for air content reduction and grout penetration into the crevices, avoiding disturbance to the samples specially in the first 10 hours of casting, etc.
8. It is recommended to do a test without the top cap to inflict a top-end effect and compare the previous study results. In the field, both the top and bottom part of a grout element are constrained; one by the bond to the rock and the other by a bond to the cable. This will call to a experiment where end effect is inflicted on both sides of the sample, contrary to this study where the top surface was free for lateral expansion. Also, this can be even further extended by providing confinement to the sample.

ACKNOWLEDGEMENT

Authors' would like to acknowledge the ongoing *in-kind* support of MINOVA, in particular Mr Robert Hawker, for this research study.

REFERENCES

- Aziz, N, Jalaifar, H, and Concalves, J, 2006 'Bolt Surface Configurations and Load Transfer Mechanism, in Naj Aziz and Bob Kininmonth (eds.), Proceedings of the 2006 Coal Operators' Conference', Mining Engineering, University of Wollongong, 18-20 February 2006, <https://ro.uow.edu.au/coal/51>
- Bajwa, PS, Hagan, P, and Li, D, 2019, ' A comparison between resin and a cementitious material in the grouting of cable bolts, in Naj Aziz and Bob Kininmonth (eds.), Proceedings of the 2017 Coal Operators' Conference, Mining Engineering, University of Wollongong, 18-20 February 2019. <https://ro.ouw.edu.au/coal/642>
- Cao, C, Nemcik, J, Aziz, N, and Ren, T, 2013, '*Dilatational slip angle of rebar bolts under axial loading*, ' 13th Coal Operators Conference., University of Wollongong, The Australasian Institute of Mining and Metallurgy & Mine Managers Association of Australia, 2013, pp 156-162.

- Chen, Y., and Li, C.C., 2014, 'Performance of fully encapsulated rebar bolts and D-bolts under combined pul-and-shear loading,' *Tunnelling and Underground Space Technology* Vol 45, January 2015, pp 99-106
- Craig, P, and Holden, M, 2014, 'In-situ bond strength testing of Australian cable bolts,' *14th Coal Operators' Conference*, University of Wollongong, The Australasian Institute of Mining and Metallurgy & Mine Managers Associations of Australia, 2014, pp 147-155.
- Hagan, P, Chen, J, and Saydam, S, 2019, 'The load transfer mechanism of fully grouted cable bolts under laboratory test, in Naj Aziz and Bob Kininmonth (eds.), *Proceedings of the 2014 Coal Operators' Conference*', Mining Engineering, University of Wollongong, 18-20 February 2019, <https://ro.uow.edu.au/coal/507>
- Hoek, E, 2007, 'Practical Rock Engineering,' 2007 edn, Rocscience Inc, Toronto, viewed 30 March 2020, <https://www.rocscience.com/assets/resources/learning/hoek/Practical-Rock-Engineering-Full-Text.pdf>
- Hutchinson, J, and Diederichs, M, 1996, 'Cablebolting in Underground Mines', BiTech Publishers Ltd., Canada.
- Hyett, A, Bawden W, and Reichert, R, 1992, 'The effect of rock mass confinement on the bond strength of fully grouted cable bolts, *Int. J. Rock mechanics and Min. Sci.& Geomech. Abstr.*, 29(5), pp 503-524.
- Majoor, D, Mirzaghobanali, A, and Aziz, N, 2019, *Strength properties of grout for strata reinforcement*, in Naj Aziz and Bob Kininmonth (eds.), *Proceedings of the 2017 Coal Operators' Conference*, Mining Engineering, University of Wollongong, 18-20 February 2019, <https://ro.uow.edu.au/coal/641>
- McTyer, K, and Evans, DW, 2017, 'Mechanical direct shear tests of cables – combined stress relationships,' *Proceedings of the 17th Coal Operators Conference.*, Mining Engineering, University of Wollongong, 8-10 February 2017, pp 171-182.
- Mirza, A, Aziz, N, Ye, W, and Nemcik, J, 2016, 'Mechanical Properties of Grouts at Various Curing Times,' *Proceedings of the 16th Coal Operators Conference*. Mining Engineering, University of Wollongong, February 2018, pp 343-352. <https://ro.uow.edu.au/coal/714>
- Mirzaghobanali, A, Gregor P, Alkandari, H, Aziz, A, and McDougall, K, 2019, 'Mechanical Behaviours of Grout for Strata Reinforcement, in Naj Aziz and Bob Kininmonth (eds.), *Proceedings of the 2018 Coal Operators' Conference*', Mining Engineering, University of Wollongong, 18-20 February 2019, <https://ro.uow.edu.au/coal/717>
- Mirzaghobanali, A, Gregor, P, Ebrahim, Z, Alfahed, A, Aziz, A and McDougall, K, 2019, 'Strength properties of grout for strata reinforcement, in Naj Aziz and Bob Kininmonth (eds.), *Proceedings of the 2019 Coal Operators Conference*', Mining Engineering, University of Wollongong, 18-20 February 2019, 196-202.
- Pells, P, and Bertuzzi, R, 1999, 'Permanent Rockbolts – The Problems are in the Detail,' *Tenth Australian Tunnelling Conference 1999*. Melbourne, Victoria, 21-24 March 1999, pp 255-259.
- Potvin, Y, Hudyma, M, and Miller, H.D.S., 1989, 'Design guidelines for open stope support,' *CIM Bulletin* 82, June 1989, pp 53-62.
- Pullan, E, Li, D, and Hagan, PC, 2019, 'Comparison of the Performance of Resin and Cementitious Grout Media for Cable Bolts, in Naj Aziz and Bob Kininmonth (eds.), *Proceedings of the 2018 Coal Operators' Conference*', Mining Engineering, University of Wollongong, 18-20 February 2019, <https://ro.uow.edu.au/coal/716>
- Yang, G, Aziz, N, Rasekh, H, Khaleghparast, S, Li, X, and Nemcik, J, 2018 February, 'Profile of Sheared Cable Bolts Strand Wires,' *Proceedings of the 18th Coal Operators Conference*. Mining Engineering, University of Wollongong, February 2018, pp 343-352. <https://ro.uow.edu.au/coal/714>
- Zhang, C, Cui, G, Chen, X, Zhou, H, and Deng, L, 2020 January, 'Effects of bolt profile and grout mixture on shearing behaviors of bolt-grout interface,' *Journal of Rock Mechanics and Geotechnical Engineering* 12(2020), 23 January 2020, pp 242-255.
- Zohaib, M, Mirzaghobanali, A, Helwig, A, Aziz, Gregor, P, Rastegarmanesh, A and McDougall, K, 2020 February, 'Shear Strength Properties of Artificial Rock Joints,' *Proceedings of the 2020 Coal Operators Conference (2020)*. Coal Operators' Conference. 757. pp 32 – 44, <https://ro.uow.edu.au/coal/757>